Current and efficiency optimization under oscillating forces in entropic barriers*

Ferhat Nutku† and Ekrem Aydıner

Theoretical Physics Research Group, Department of Physics, Faculty of Science, İstanbul University, Vezneciler, İstanbul 34134, *Turkey*

(Received 17 February 2016; revised manuscript received 7 May 2016; published online 2 August 2016)

The transport of externally overdriven particles confined in entropic barriers is investigated under various types of oscillating and temporal forces. Temperature, load, and amplitude dependence of the particle current and energy conversion efficiency are investigated in three dimensions. For oscillating forces, the optimized temperature–load, amplitude–temperature, and amplitude–load intervals are determined when fixing the amplitude, load, and temperature, respectively. By using three-dimensional plots rather than two-dimensional ones, it is clearly shown that oscillating forces provide more efficiency compared with a temporal one in specified optimized parameter regions. Furthermore, the dependency of efficiency to the angle between the unbiased driving force and a constant force is investigated and an asymmetric angular dependence is found for all types of forces. Finally, it is shown that oscillating forces with a high amplitude and under a moderate load lead to higher efficiencies than a temporal force at both low and high temperatures for the entire range of contact angle.

Keywords: entropic barrier, Brownian motion, Fick–Jacobs equation, efficiency of Brownian motor

PACS: 05.40.Jc, 05.10.Gg, 05.40.–a **DOI:** 10.1088/1674-1056/25/9/090501

1. Introduction

In the entropic barriers, non-equilibrium thermal fluctuations are caused by the heat transfer between the system and the background heat bath combined with the asymmetric shape of a channel which can lead to a unidirectional particle current. These systems are so called thermal ratchets or Brownian motors in the literature.[1–3] Understanding of Brownian motion in the entropic or energetic barriers plays an important role in the biological systems. For example, the migration of living cells usually has been explained by the laws of Brownian motion.[4] On the other hand, entropic barriers are used to separate dispersed particles from a suspension fluid. DNA separation,[5,6] particle diode,[3,7–9] and separation of particles according to their sizes[10–12] are common examples of utilizing entropic barriers in technological applications.

Theoretically, particle transport has been studied under different restrictive potentials such as energetic ratchet,[13,14] periodically rocked ratchet,[15,16] horizontally oscillating inclined ratchets,[17] entropic barriers,[18–23] flashing barriers,[24] and oscillating entropic barriers.[25–27] For example, Ai *et al.*[19,20] showed that a net diffusion current and optimized efficiency exist in the presence of a periodic, unbiased, having zero mean, and temporally symmetric external driving force although the average of acting unbiased driving force and random thermal noise are zero. In a recent work, Reguera and Rubi[23] discussed how to optimize the shape of an entropic barrier. It is shown that by applying an external driving force with a high amplitude and choosing an appropriate barrier shape, a higher effective diffusion coefficient compared with the free particle diffusion coefficient can be achieved. In such a mechanism, the drift against an external force can be suppressed and a directed particle transport can be obtained in a confining entropic tube. They emphasized that an unbiased external driving force and an optimized barrier shape can lead to possible applications in particle separation and mixing of colloidal solutions. Sumithra *et al.*[13] showed that, in forced ratchets driven by oscillating forces, efficiency can be optimized due to thermal fluctuations. Dan *et al.*[16] investigated the effect of spatially periodic friction on the average of the particle current in a rocked ratchet. They assumed space-dependent friction coefficient as $\gamma(x) = \gamma_0(1 - \lambda\sin(x+\phi))$ and a ratchet potential as $V(x) = V_0(x) + fx$ where V_0 is a spatially periodic function such that $V_0(x+2\pi n) = V_0(x) = -\sin(x)$, f is the slope of the potential which represents the load, ϕ is the phase difference between the $V_0(x)$ and the friction. They have chosen a square wave force and calculated the average of the particle current and efficiency. In other work, Dan *et al.*[14] studied temperature dependence of the efficiency for an energetic ratchet with an asymmetric potential $V(x) = -1/(2\pi)[\sin(2\pi x) + \Delta/4\sin(4\pi x)] + fx$ where f is the external load, and Δ is the asymmetry parameter with a value in the range 0–1. In their work, the system is rocked by a periodic oscillating force with the form of $F(t) = A\sin(\omega t)$. Moreover, current and efficiency in different entropic barrier models have been intensively investigated by using an oscillating force in Refs. [12], [21], [22], [26], and [27]. Especially, Burada *et al.*[21,22] studied entropic stochastic res-

*Project supported by the Istanbul University, Turkey (Grant No. 55383).

†Corresponding author. E-mail: fnutku@istanbul.edu.tr

© 2016 Chinese Physical Society and IOP Publishing Ltd

onance which is the phenomenon of interference of thermal noise with an entropic barrier and driving force via Brownian particles. In this model, boundaries which confine the motion of Brownian particles are chosen as a dumb bell shape given by $\omega_{\pm}(x) = L_y(x/L_x)^4 - 2L_y(x/L_x)^2 - b/2$ where $\pm$ denote upper and lower branches of the boundaries, L_x and L_y respectively define the horizontal and vertical distances between the widest and narrowest parts of the dumb bell, and b is the width of the smallest vertical opening of the structure. They showed that the resonance behavior has been found when a sinusoidal time-dependent oscillating force was applied along the horizontal axis of the confining barrier and spectral amplification was related to the parameters of the sinusoidal driving force. On the other hand, an asymmetric sawtooth potential has been considered in order to separate the Brownian particles in Refs. [12] and [26]. In these works, Reguera *et al.*[12] showed that by applying a periodic square wave force, particles of different radii can be separated and forced to be accumulated at the left and right hand sides of the channel. Kalinay[26] studied rectification of the particle current where particles are confined in a sinusoidally rocked $F(t) = F_0\cos(\omega t)$ asymmetric sawtooth like channel and found that current rectification is proportional to the square of the amplitude ($\sim F_0^2$). Additionally, in Ref. [28] the current and efficiency of Brownian particles in the entropic barrier have been investigated by using various types of oscillating forces.

In recent studies, in order to determine the effective diffusion coefficient in 2D periodic channels, Kalinay[29] used a different approach by formulating the transport problem in a complex plane and applying Fourier's analysis. In a further study, Kalinay[30] generalized his approach in Ref. [29] by applying functional analysis to three-dimensional (3D) channels of cylindrical symmetry where particles are driven by a constant longitudinal external driving force. In this approach, the investigation of effective diffusion constant is done without homogenizing and reducing the motion to one-dimensional (1D), which can also enable one to explore transport in corrugated structures.

As it is seen from previous studies that the main problem in both theoretical and experimental studies is to determine the parameter regions which give the maximal efficiency. In most of recent studies, the current and efficiency of entropic barrier models have been studied for a single fixed parameter for a temporal and/or an oscillating force. These cases give limited information for the optimized parameter region. However, understanding the optimized parameter region which gives maximal efficiency can provide valuable information to the experimental studies. Therefore, in this work, based on our previous study[28] we have comprehensively investigated the parameter dependence of the current and efficiency by plotting three-dimensional figures. Additionally, we have obtained results for various oscillating forces and compared with that of a temporal force. By investigating three-dimensional plots, we determined the optimized temperature–load, amplitude–temperature, and amplitude–load intervals. We have also showed that three-dimensional plots provide more information to determine the maximal current and efficiency regions than two-dimensional plots. Finally, we have compared angular dependence of the efficiency for oscillating and temporal forces by employing the angle between the load and driving force, which were changed between 0–π. These improvements in this study can enlighten and/or guide experimental researches studying on biological, fluidic systems at nano- and microscales.

The paper is organized as follows. In Section 2, we give theoretical background and mathematical formulation of current and efficiency of Brownian particles in an entropic barrier. In Section 3, we present the model of entropic barrier and oscillating force. In Section 4, numerical results are given. Finally, in Section 5, we briefly conclude the importance of the obtained results.

2. Theoretical background

In order to discuss the current and efficiency in a Brownian motor, an ensemble of Brownian particles which are suspended in a carrier medium, under periodic, symmetric unbiased external forces applied along the horizontal direction should be considered. In three dimensions, this motion can be described by the following overdamped Langevin equations:

$$\frac{\mathrm{d}x}{\mathrm{d}t} = \frac{F(t)-f}{\gamma} + \sqrt{D_0}\xi_x(t), \tag{1}$$

$$\frac{\mathrm{d}y}{\mathrm{d}t} = \sqrt{D_0}\xi_y(t), \tag{2}$$

$$\frac{\mathrm{d}z}{\mathrm{d}t} = \sqrt{D_0}\xi_z(t), \tag{3}$$

where x, y, and z are the three-dimensional coordinates, γ is the friction coefficient, $F(t)$ is the externally applied time-dependent force, f is the constant load, D_0 is the diffusion coefficient of unconfined free particles given as $D_0 = k_{\mathrm{B}}T/\gamma$, k_{B} is the Boltzmann constant, T is the temperature, ξ_x, ξ_y, and ξ_z are the independent Gaussian white noise distributions, which have zero mean and satisfy the correlation function, $\langle\xi_i(t)\xi_j(t')\rangle = 2\delta_{ij}\delta(t-t')$ for $i,j = x,y,z$. Here, brackets denote the ensemble average and $\delta(t)$ is the Dirac delta function. It is worth mentioning that, due to the high viscosity, one can obtain the overdamped Langevin equation by setting acceleration equal to zero.

The 3D or 2D motion of Brownian particles can be reduced to 1D which is along the x axis by elimination of the y and z coordinates in the 3D or 2D Smoluchowski equation.[18,31] This derivation will lead to a modified Fick–Jacobs equation

$$\frac{\partial P(x,t)}{\partial t} = \frac{\partial}{\partial x}\left(D(x)\frac{\partial P(x,t)}{\partial x} + \frac{D(x)}{k_{\mathrm{B}}T}\frac{\partial A(x,t)}{\partial x}P(x,t)\right), \tag{4}$$

where $P(x,t)$ is the probability density for the particle at the x position at time t. Here, $D(x)$ is the effective diffusion coefficient proposed by Reguera and Rubi[18] given in the following:

$$D(x) = \frac{D_0}{\left[1+\left(\frac{\mathrm{d}\omega(x)}{\mathrm{d}x}\right)^2\right]^{\alpha}}, \tag{5}$$

where D_0 is the free particle diffusion coefficient mentioned above, $\omega(x)$ is the radius of entropic barrier that forms a tube structure in 3D or half width of the channel formed in 2D. Here, $\alpha = 1/3,\ 1/2$ are scaled exponents used in 2D or 3D, respectively. According to their reasoning, the diffusion coefficient includes displacements both in horizontal and vertical directions. Mathematically, this thought can be represented with a derivative of the shape of the enclosure. In addition, by including scaling exponents, Reguera and Rubi have obtained an approximation to the diffusion coefficient. Their effective diffusion coefficient is in an excellent agreement with the exact solution of the Smoluchowski equation when compared to the Zwanzig's effective diffusion coefficient.[18] In the Fick–Jacobs equation, $A(x,t)$ is the free energy defined by $A(x,t) = U - TS$, $U = fx - F(t)x$ is the internal energy, $S = k_{\mathrm{B}} \ln h(x)$ is the entropy, $h(x)$ corresponds to the dimensionless width of the tube in 2D and transverse cross section of the tube in 3D and it is given as

$$h(x) = \begin{cases} \dfrac{2\omega(x)}{L}, & \text{2D}, \\ \pi\left(\dfrac{\omega(x)}{L}\right)^2, & \text{3D}. \end{cases} \tag{6}$$

Investigating Brownian transport by the above explained entropic scheme simplifies the complexity of the dynamics and reduces the governing equations of motion defined in 3D or 2D to a single 1D equation.

The Fick–Jacobs equation can be considered as a special form of the Fokker–Planck equation, which accounts for the time evolution of the probability density along the x direction. In general, the Fokker–Planck equation relates the time evolution of the probability distribution $P(x,t)$ with the probability current density $j(x,t)$, in the following:

$$\frac{\partial P(x,t)}{\partial t} = -\frac{\partial j(x,t)}{\partial x}, \tag{7}$$

where $j(x,t)$ is given in the following:

$$j(x,t) = -D(x)\,\mathrm{e}^{-\beta A(x)}\frac{\partial}{\partial x}\left\{\mathrm{e}^{\beta A(x)}P(x,t)\right\}. \tag{8}$$

Ai *et al.*[20] derived an expression of the particle probability current for particles confined in entropic barriers by using the mean first-passage time approach, which is also presented in Refs. [31] and [32]. In this method, overdamped stochactic Langevin equations of motion of particles in 3D or 2D are reduced to 1D by using the Fokker–Planck equation for the probability distribution of particles under the Ficks–Jacobs approximation. The current is given by

$$j(t,\theta) = \frac{k_{\mathrm{B}}T\left[1-\exp\left(-\dfrac{(F(t)+f\cos\theta)L}{k_{\mathrm{B}}T}\right)\right]}{\int_0^L h(x)\exp\left(\dfrac{(F(t)+f\cos\theta)x}{k_{\mathrm{B}}T}\right)\kappa\,\mathrm{d}x}, \tag{9}$$

where κ is

$$\kappa = \int_x^{x+L}\left[1+\left(\frac{\mathrm{d}\omega(y)}{\mathrm{d}x}\right)^2\right]^{\alpha} h^{-1}(y) \times \exp\left(-\frac{(F(t)+f\cos\theta)y}{k_{\mathrm{B}}T}\right)\mathrm{d}y,$$

and k_{B} is Boltzmann's constant, T is the temperature, $F(t)$ is the external driving force, f is the constant force, θ is the angle between the driving and constant force, and $h(x)$ is the dimensionless width of the channel, which is given in three dimensions with $h(x) = \pi(\omega(x)/L)^2$.

Finally, the mean average current per period in the entropic barriers can be computed by the following integration:

$$\langle J\rangle = \frac{1}{\tau}\int_0^{\tau} j(t)\,\mathrm{d}t. \tag{10}$$

The investigated potential V only depends on x and satisfies the periodic boundary conditions as $V(x,t+\tau) = V(x,t)$ and $V(x+L,t) = V(x,t)$ so the efficiency can be given as[17]

$$\eta = \frac{\langle W\rangle}{\langle E_{\mathrm{in}}\rangle} = \frac{\frac{f}{\tau}\int_0^{\tau}\mathrm{d}t\int_0^{L}\mathrm{d}x\,j(x,t)}{\frac{1}{\tau}\int_0^{\tau}\mathrm{d}t\int_0^{L}\mathrm{d}x F(t)j(x,t)}. \tag{11}$$

At this point, it is important to mention that the reduction from the Smoluchowski equation to the so called Fick–Jacobs approximation is invalid under strong forcing, wrinkled or trapped barriers. Moreover, the Fick–Jacobs approximation relies on the assumption of faster equilibration in the transverse direction than in the longitudinal transport direction. The Fick–Jacobs approximation is valid if the relaxation time of the motion along the vertical axis is much smaller than the relaxation time along the horizontal axis $\tau_y \ll \tau_x$. Barrier geometry must satisfy the $|\mathrm{d}\omega(x)/\mathrm{d}x| \ll 1$ condition. We have checked the validity of the Fick–Jacobs approximation in our previous work for the same entropic barrier geometry and parameters and found that they satisfy the global criteria for the validity of the Ficks–Jacobs description.[28] More information on local and global criteria for the validity of the Fick–Jacobs description and dimensionless scaling parameter can be found in Refs. [31] and [32]

An additional criterion has been proposed by Dagdug *et al.*[33] for effective diffusion coefficient D_{eff} of Brownian motion in periodic tubes with corrugated walls. In corrugated periodic tubes, the characteristic length L/a of the radius variation must be larger enough than 1 for using the approximate effective diffusion coefficient and in our study the $L/a = 4\pi > 1$ inequality is satisfied. As the corrugation of an entropic tube

decreases and the shape of the tube becomes as a linear channel $D_{\rm eff}/D_0$ ratio becomes one. Recently, applicability of the one-dimensional reduction of the Brownian transport via entropy potentials has also been reviewed in Ref. [34].

In our work, the frequency of force is kept constant and small in order to provide faster equilibration along the vertical direction than the horizontal direction. Average current expression (Eq.(10)) derived under the Fick–Jacobs approximation will give the same results for forces with different oscillation frequencies. Because all investigated forces are unbiased and have a zero-mean value when integrated over time. The difference between current and efficiency under various types of forces might arise from the difference of space–time correlation between driving force $F(t)$ and barrier geometry $\omega(x)$. In the literature, the impact of the frequency of oscillating driving force, which is applied at one end of a particle chain, on the mean velocity of Brownian particles interacting with each other via the Morse potential and under an asymmetric periodic potential have been investigated in Ref. [9]. In their work, Ai *et al.* integrated equations of motion for overdamped and underdamped cases by the second-order stochastic Runge–Kutta method. According to their results, a particle diode can be built by changing the frequency of driving force.

3. The model

Geometry of the entropic tube plays an essential role in the transport of the particles. In this work, in order to make comparisons with results obtained in the literature, barrier shape is selected to be the same as that given in Ref. [20]

$$\omega(x) = a\left[\sin\left(\frac{2\pi}{L}(x-\phi)\right) + \frac{\Delta}{4}\sin\left(\frac{4\pi}{L}(x-\phi)\right)\right] + b, \quad (12)$$

where a is the amplitude of the barrier, b determines the half width at the bottleneck of the tube, L is the length of one period of the tube, Δ is a parameter which defines the asymmetry of the tube and $\omega(x)$ defines the half width of the tube. Selected parameters are $a = 1/2\pi$, $b = 1.5/2\pi$, $\Delta = 1.0$, $L = 2\pi$. A phase angle $\phi = \tan^{-1}\left(\sqrt{2}\sqrt[4]{3}/(\sqrt{3}-1)\right)$ is subtracted from the argument value x in order to match the periodicity of the external force and the periodicity of the barrier. This spatial translation removes the phase difference between the force and the barrier. In this way, spatial and temporal variables are matched at the same scale for space $L = 2\pi$ and time $\tau = 2\pi$ as seen in Fig. 1.

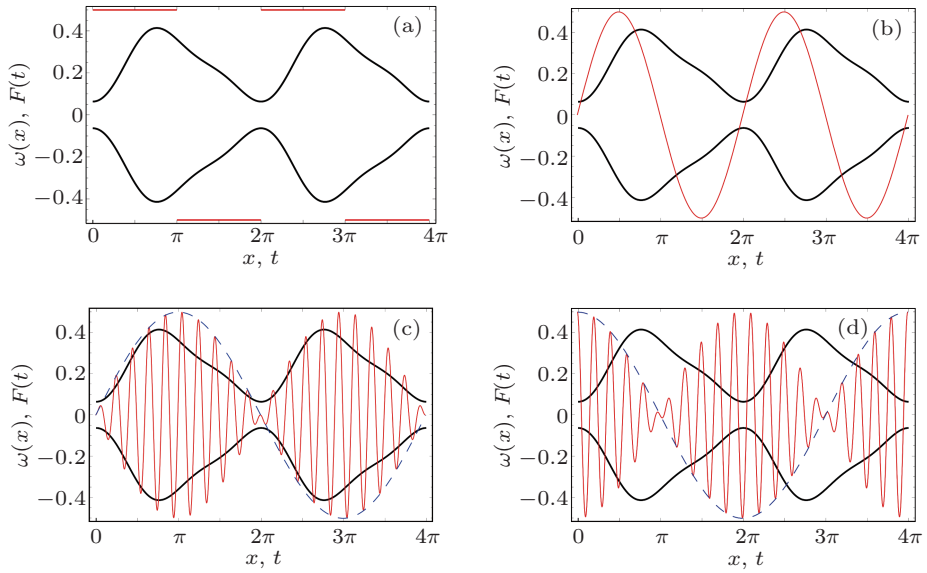


Fig. 1. (color online) Two periods of the entropic barrier under unbiased temporal (a), sinusoidal (b), amplitude modulated sinusoidal (c), amplitude modulated cosinusoidal (d) forces (force is drawn in red color, the blue-dashed line presents the envelope of the amplitude).

In this work, we investigated four different types of external driving forces given as follows:

$$F(t) = \begin{cases} A, & n\tau \le t < n\tau + \dfrac{1}{2}\tau, \\ -A, & n\tau + \dfrac{1}{2}\tau < t \le (n+1)\tau, \end{cases} \quad (13)$$

$$F(t) = A\sin(t), \quad (14)$$

$$F(t) = A\sin(t/2)\sin(10t), \quad (15)$$

$$F(t) = A\cos(t/2)\cos(10t). \quad (16)$$

These forces are exerted to Brownian particles inside the entropic barriers. All of them are unbiased and periodic forces. They are constant in space, but variable in time and directed along the horizontal axis of the channel. Two periods of the asymmetric barrier and profiles of the applied forces are depicted in Fig. 1, where the amplitude change of modulated forces are enveloped by blue-dashed lines.

4. Results and discussion

In order to present the current and efficiency changes, three-dimensional plots of temperature–load–current (T–f–J), temperature–load–efficiency (T–f–η), amplitude–temperature–current (A–T–J), amplitude–temperature–efficiency (A–T–η), amplitude–load–current (A–f–J) and amplitude–load–efficiency (A–f–η) are plotted. In these calculations, the angle θ between the stimulating force $F(t)$ and constant force f is set to π. Therefore, the constant force behaves like a load.

In the temperature–load–efficiency plot which is given in Fig. 2(a) for constant amplitude $|A| = 0.5$, at moderate temperature and moderate load, efficiency is maximum. Increasing temperature and load decreases both current and efficiency under all types of driving forces. The highest current and efficiency is obtained in a low temperature and load region. In 3D plots, the color seen on top of other layers has the highest value. At amplitude $|A| = 0.5$, temporal force provides both higher current and efficiency when it is compared with oscillating forces. The temperature–load–current change is given in Fig. 2(b). As it can be seen from the figure the current increases with the increase of temperature; however, after it reaches up to a maximum, and then it smoothly deceases at low load values. In temperature–load–efficiency plots, the plot belonging to cosinusoidally amplitude modulated force (Eq. (16)), which is in yellow color, totally overlaps with that of sinusoidally amplitude modulated force (Eq. (15)), so its color cannot be distinguishable. Overlapping of current and efficiency calculated sinusoidally and cosinusoidally modulated oscillating forces are also presented in our previous work.[28] This overlap is destroyed above a critical amplitude and a separation in current and efficiency occurs between sinusoidally and cosinusoidally modulated oscillating forces, as it is clearly seen in Figs. 3(a), 3(b), and 4(a). Further investigation is needed for understanding the physical background of this difference. One useful method might be relating barrier shape $\omega(x)$ with driving force $F(t)$ by calculating the space–time correlation function. After this calculation, it might be expected that although time averages of sinusoidally and cosinusoidally modulated functions are the same and zero, their correlations with barrier shape are different. As a result, different types of driving forces lead to different current and efficiencies.

In the amplitude–temperature–efficiency plot given in Fig. 3(a), for a constant load $f = 0.01$, the efficiency is maximum at the low temperature and low amplitude region. Increasing the amplitude decreases the efficiency under all types of forces especially for the temporal force. On the other hand, in a high amplitude and high temperature region, the efficiency of the Brownian motor under oscillating forces is higher than that of temporal force, as seen in Fig. 3(a). The amplitude–temperature–current plot is given in Fig. 3(b). As seen in this figure, when increasing the amplitude and temperature, the current increases under all types of forces. A higher current can be obtained by applying oscillating forces at a low temperature and high amplitude region. When the temperature is increased, above a critical value, a crossover occurs and under a temporal force, the current becomes higher than that of oscillating forces, as seen in Fig. 3(b).

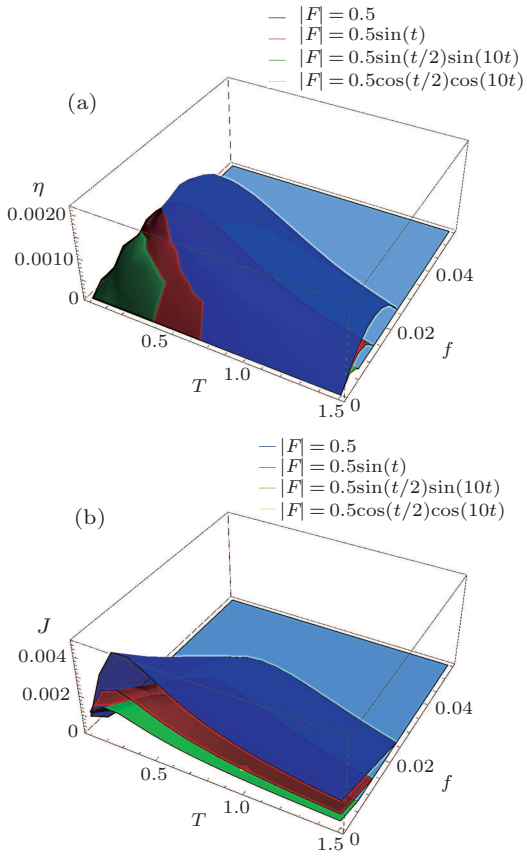


Fig. 2. (color online) Temperature–load–efficiency (a), temperature–load–current (b) plots of the investigated Brownian motor under an amplitude of ($A = 0.5$). Sinusoidally and cosinusoidally modulated forces overlap, the yellow colored one is indistinguishable from the green colored one.

Figure 4(a) shows the amplitude–load–efficiency plot at constant temperature $T = 0.5$. As it can be seen, the efficiency has high values in a vast amplitude–load region. Increasing the amplitude and load, the efficiency decreases under all types of force. As seen in Fig. 4(b), the change of the current with respect to the amplitude and load is interesting. Increasing the amplitude of the driving force up to a critical value increases the current. But above a critical amplitude, the driving force adversely affects the particle transport, which causes the current to decrease. Referring to Figs. 4(a) and 4(b) after increasing the amplitude above a critical value, the current and efficiency under oscillating forces become higher when compared with those of a temporal force. As previously mentioned in a special A–T region in Figs. 3(a) and 3(b) and A–f region in Fig. 4(a) oscillating force with cosinusoidal amplitude modulation gives different efficiency and current when compared with sinusoidal amplitude modulation. The presented three-dimensional results are consistent with the 2D ones obtained in our previous work.[28]

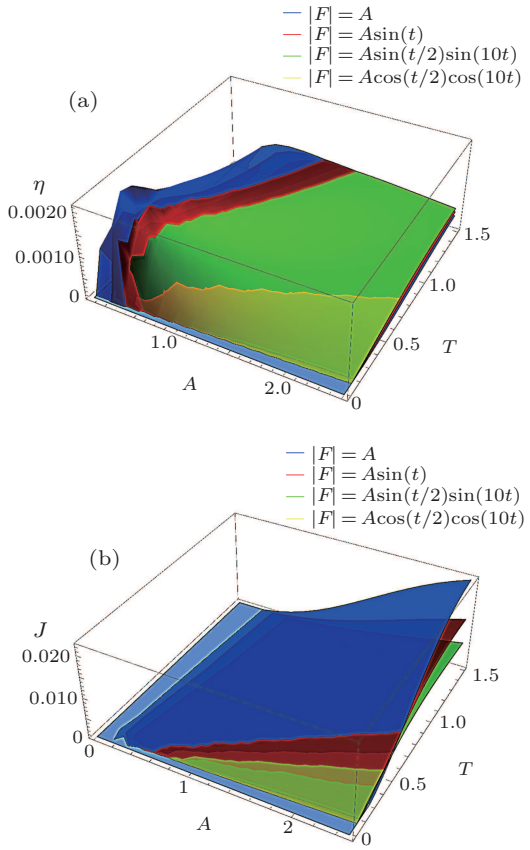


Fig. 3. (color online) Amplitude–temperature–efficiency plot (a) and amplitude–temperature–current plot (b) of the investigated Brownian motor at constant load ($f = 0.01$).

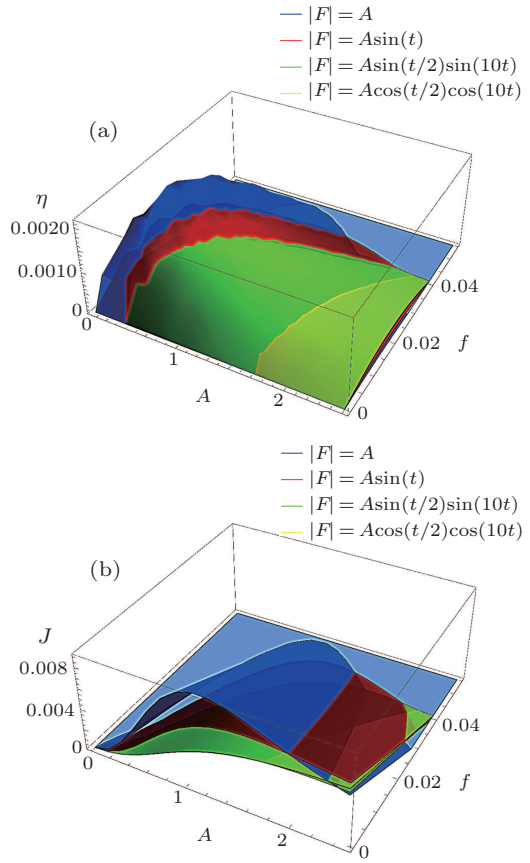


Fig. 4. (color online) Amplitude–load–efficiency plot (a) and amplitude–load–current plot (b) of the investigated Brownian motor at constant temperature ($T = 0.5$).

Furthermore, in order to reveal the effect of the direction of a constant force, the angle between the driving force $F(t)$ and the constant force f changes between 0 and 2π. If the angle is $\theta = \pi$ in Eq. (9), then f represents a constant frictional force, in other words a constant load, but if $\theta = 0$ in Eq. (9), then f can be treated as a constant facilitating drift force applied to Brownian particles. Since we are applying the Fick–Jacobs approximation and assuming a faster equilibration in the transverse direction than in the longitudinal transport, only the x component of the load is considered in calculations. An interesting result is found when a drift force $f = 0.01$, $\theta = 0$ is superimposed to the driving force with amplitude $A = 0.5$ and 1.5 at $T = 0.5$ and 1. Although efficiency is higher for the temporal force at $\theta = \pi$ (friction case) at $T = 0.5$ and 1 (see Figs. 5(a) and 6(a)), under oscillating forces with amplitudes $A = 0.5$ and 1.5 at $\theta = 0$ (drift case) efficiency is higher than that of temporal force at all temperatures as seen in Figs. 5(a) and 5(b) and Figs. 6(a) and 6(b). At temperature $T = 0.5$, when the amplitude is increased up to $A = 1.5$, again under a constant friction force $f = 0.01$, the efficiency is higher under oscillating forces as seen in Fig. 5(b). Polar plots of efficiency calculations presented in Figs. 5(a) and 5(b) are consistent with the results plotted in 3D shown in Fig. 3(a).

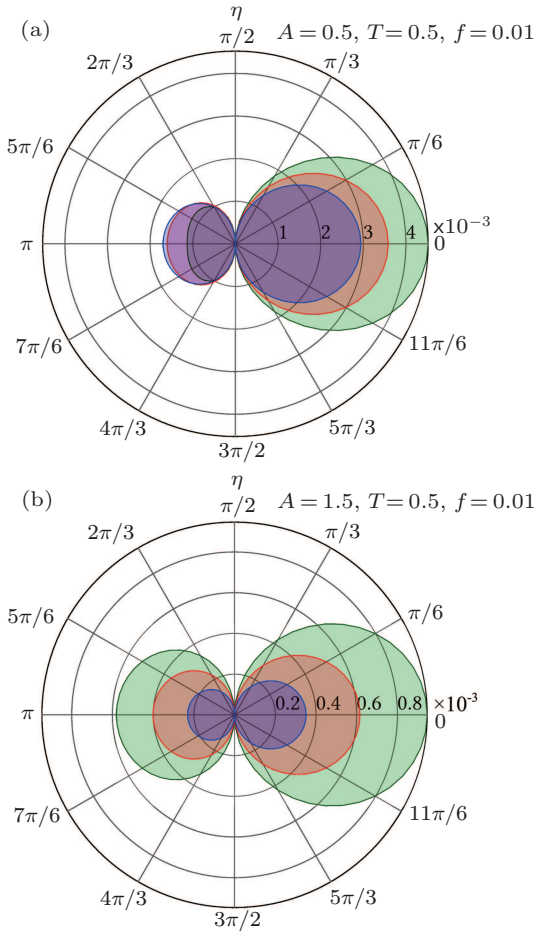


Fig. 5. (color online) Efficiency η versus load direction under various types of forces $A = 0.5$ (a) and $A = 1.5$ (b) at $T = 0.5$, $f = 0.01$ (low temperature case). Blue, red, green colors represent results for forces given by Eqs. (13)–(15), respectively.

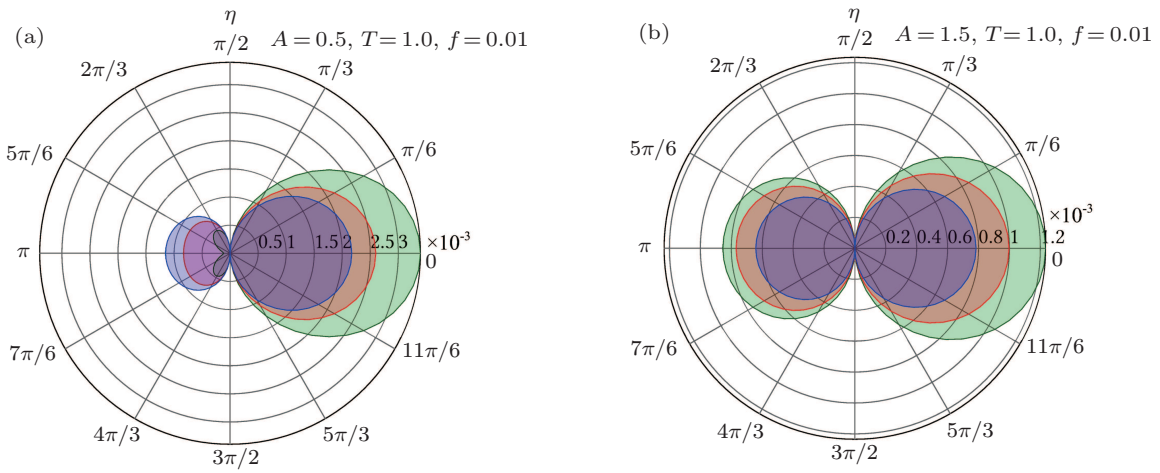


Fig. 6. (color online) Efficiency η versus load direction under various types of forces $A = 0.5$ (a), $A = 1.5$ (b) at $T = 1.0$, $f = 0.01$ (high temperature case). Blue, red, green colors represent results for forces given by Eqs. (13)–(15), respectively.

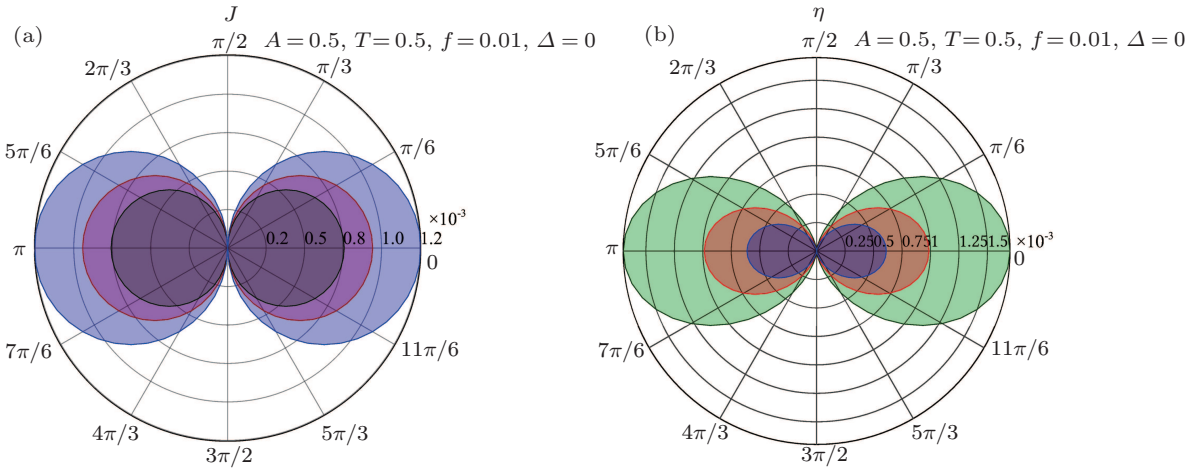


Fig. 7. (color online) Current J (a) and efficiency η (b) versus load direction under various types of forces with parameters $A = 0.5, T = 0.5, f = 0.01$ inside a symmetric barrier with $\Delta = 0$. Blue, red, and green colors represent results for forces given by Eqs. (13)–(15), respectively.

These plots reveal to us the directed transport of Brownian particles. Physically, the asymmetry in the polar plots arises from the parameter Δ, which defines the asymmetry of the entropic tube. This Δ parameter, which breaks the symmetry along the x axis, causes the entropic barrier to lead the particles to become transported in a preferential direction. When the Δ parameter is set to zero, under $A = 0.5$, $T = 0.5$, $f = 0.01$ conditions, angular dependence of the current and efficiency becomes symmetric, as seen in Figs. 7(a) and 7(b). In this case the barrier shape is symmetric along the x axis, which prevents a directed net motion if additionally constant force f is set to zero.

5. Concluding remarks

The current and energy conversion efficiency of particle transport in entropic barriers is studied three dimensionally by fixing one of the parameters such as amplitude, load, or temperature and changing the other parameters such as temperature–load, amplitude–temperature, or amplitude–load, respectively. This type of three-dimensional study enables one to specify optimized parameter regions more explicitly than two-dimensional studies. Indeed, it is shown that three-dimensional plots clearly reveal that in the case of particle transport inside an asymmetric entropic tube, the external force which supplies the highest particle current does not necessarily give the highest efficiency. The efficiency is a function of the temperature, load, and amplitude of the driving force. In order to obtain the highest efficiency, one should determine the optimized temperature, load, and amplitude ranges for each type of unbiased force defined by a certain time dependency: according to three-dimensional plots, under a moderate constant load, at high amplitudes and high temperatures; at a moderate constant temperature, at high amplitudes and high loads, oscillating forces give higher efficiencies than temporal force.

Additionally, in polar plots, the change of the efficiency with respect to the angle between the constant load/drift force is investigated. It is seen that efficiency values and their angular distributions obtained under oscillating forces are different to those under the temporal force. In the high amplitude case, when there is a constant load, oscillating forces give higher efficiencies than the temporal force at both low and high temper-

atures for every angle. If the barrier parameter Δ is set to zero, the barrier shape becomes symmetric along the x axis, the angular dependence of efficiency and current becomes symmetric.

In summary, we reconsider that utilizing oscillating unbiased driving forces inside entropic tubes can provide an extra flexibility for dynamically controlling the particle current and energy conversion efficiency, and we show that a three-dimensional study enables one to specify optimized parameter regions more explicitly than two-dimensional studies.

References

[1] Reimann P 2002 *Phys. Rep.* **361** 57
[2] Parrondo J and de Cisneros B 2002 *Appl. Phys. A: Mater. Sci. & Process.* **75** 179
[3] Hänggi P 2009 *Rev. Modern Phys.* **81** 387
[4] Tsekov R and Lensen M C 2013 *Chin. Phys. Lett.* **30** 070501
[5] Han J and Craighead H G 2000 *Science* **288** 1026
[6] Streek M, Schmid F, Duong T T and Ros A 2004 *J. Biotechnol.* **112** 79
[7] Siwy Z, Kosińska I D, Fuliński A and Martin C R 2005 *Phys. Rev. Lett.* **94** 048102
[8] Kalman E, Healy K and Siwy Z S 2007 *EPL* **78** 28002
[9] Ai B Q, He Y F and Zhong W R 2011 *Phys. Rev. E* **83** 051106
[10] Kettner C, Reimann P, Hänggi P and Müller F 2000 *Phys. Rev. E* **61** 312
[11] Müller F, Birner A, Schilling J, Gösele U, Kettner Ch and Hänggi P 2000 *Physica Status Solidi* **182** 585
[12] Reguera D, Luque A, Burada P S, Schmid G, Rubí J M and Hänggi P 2012 *Phys. Rev. Lett.* **108** 020604
[13] Sumithra K and Sintes T 2001 *Physica A* **297** 1
[14] Dan D and Jayannavar A M 2002 *Phys. Rev. E* **65** 037105
[15] Bartussek R, Hänggi P and Kissner J G 1994 *Europhys. Lett.* **28** 459
[16] Dan D, Mahato M C and Jayannavar A 2001 *Physica A* **296** 375
[17] Takagi F and Hondou T 1999 *Phys. Rev. E* **60** 4954
[18] Reguera D and Rubí J M 2001 *Phys. Rev. E* **64** 061106
[19] Ai B Q and Liu L G 2006 *Phys. Rev. E* **74** 051114
[20] Ai B Q, Xie H Z and Liu L G 2007 *Phys. Rev. E* **75** 061126
[21] Burada P, Schmid G, Reguera D, Vainstein M, Rubi J and Hänggi P 2008 *Phys. Rev. Lett.* **101** 130602
[22] Burada P S, Schmid G, Reguera D, Rubi J M and Hänggi P 2009 *EPL* **87** 50003
[23] Reguera D and Rubi J M 2014 *Eur. Phys. J. Spec. Top.* **223** 3079
[24] Ai B Q, Wang L and Liu L 2007 *Chaos, Solitons & Fractals* **34** 1265
[25] Ai B Q 2009 *J. Chem. Phys.* **131** 054111
[26] Kalinay P 2014 *Phys. Rev. E* **89** 042123
[27] Ding H, Jiang H and Hou Z 2015 *J. Chem. Phys.* **142** 194109
[28] Nutku F and Aydíner E 2015 *Chin. Phys. B* **24** 040501
[29] Kalinay P 2014 *J. Chem. Phys.* **141** 144101
[30] Kalinay P 2015 *J. Chem. Phys.* **142** 014106
[31] Burada P S, Schmid G, Reguera D, Rubí J M and Hänggi P 2007 *Phys. Rev. E* **75** 051111
[32] Reguera D, Schmid G, Burada P S, Rubi J M, Reimann P and Hänggi P 2006 *Phys. Rev. E* **96** 130603
[33] Dagdug L, Vazquez M V, Berezhkovskii A M and Bezrukov S M 2010 *J. Chem. Phys.* **133** 5
[34] Berezhkovskii A M and Bezrukov S M 2014 *Eur. Phys. J. Spec. Top.* **223** 3063